Published in final edited form as:
Cell Rep. 2012 November 29; 2(5): 1329–1339. doi:10.1016/j.celrep.2012.09.030.

Monoacylglycerol lipase is a new therapeutic target for Alzheimer's disease

Rongqing Chen[1,4], **Jian Zhang**[1,4], **Yan Wu**[1], **Dongqing Wang**[3], **Guoping Feng**[3], **Ya-Ping Tang**[2], **Zhaoqian Teng**[1], and **Chu Chen**[1]

[1]Neuroscience Center of Excellence, Louisiana State University Health New Orleans Sciences Center, New Orleans, LA 70112

[2]Department of Anatomy and Cell Biology, School of Medicine, Louisiana State University Health New Orleans Sciences Center, New Orleans, LA 70112

[3]McGovern Institute for Brain Research and Department of Brain and Cognitive Sciences, Massachusetts Institute of Technology, Cambridge, MA 02139, USA

Summary

Alzheimer's disease (AD) is the most common cause of dementia among older people. There are no effective medications currently available to prevent and treat AD and halt disease progression. Monoacylglycerol lipase (MAGL) is the primary enzyme metabolizing the endocannabinoid 2-arachidonoylglycerol in the brain. We show here that inactivation of MAGL robustly suppressed production and accumulation of β-amyloid (Aβ) associated with reduced expression of β-site amyloid precursor protein cleaving enzyme 1 (BACE1) in a mouse model of AD. MAGL inhibition also prevented neuroinflammation, decreased neurodegeneration, maintained integrity of hippocampal synaptic structure and function, and improved long-term synaptic plasticity, spatial learning and memory in AD animals. While the molecular mechanisms underlying MAGL inhibition-produced beneficial effects remain to be determined, our results suggest that MAGL, which regulates endocannabinoid and prostaglandin signaling, contributes to pathogenesis and neuropathology of AD and thus is a promising therapeutic target for the prevention and treatment of AD.

Keywords

Endocannabinoid; 2-arachidonoylglycerol; prostaglandin; β-amyloid; long-term potentiation; dendritic spines; astroglial cells; neurodegeneration; neuroinflammation; spatial learning and memory

Correspondence should be addressed to: Chu Chen, PhD, Neuroscience Center of Excellence, School of Medicine, Louisiana State University Health New Orleans Sciences Center, 2020 Gravier Street, Suite D, New Orleans, LA 70112, USA, Tel: (504) 568-8458, Fax: (504) 599-0488, cchen@lsuhsc.edu.

[4]Both authors contributed equally to this study

Statement of conflicts of interest

The authors state no conflict of interest.

Author Contributions: R.C., J.Z., Y.W. designed and performed the experiments and analyzed the data; D.W. and G.F. provided GFP-expressing transgenic mice; Y.P.T. provided the behavioral setup; Z.T. performed the experiment; and C.C. conceived the project, supervised the work, helped to design the experiments, and wrote the manuscript.

Alzheimer's disease (AD) is a neurodegenerative disorder characterized by accumulation and deposition of amyloid plaques and neurofibrillary tangles, neuroinflammation, synaptic dysfunction, progressive deterioration of cognitive function and loss of memory in association with widespread neuronal death. Over 5.4 million people in the United States and 36 million people worldwide suffer with AD in its various stages. Unfortunately, the few agents that are currently approved by the Food and Drug Administration for treatment of AD have demonstrated only modest effects in modifying the clinical symptoms for relatively short periods, and none has shown a clear effect on disease progression or prevention. Thus, there is a great public health need to discover or identify novel therapeutic targets for prevention and treatment of AD.

Monoacylglycerol lipase (MAGL) is an enzyme belonging to the serine hydrolase superfamily metabolizing lipids (Labar et al., 2009; Zechner et al., 2010), but its most striking role unveiled within this decade is in hydrolyzing the endogenous cannabinoid 2-arachidonoylglycerol (2-AG), resulting in the release of the free fatty acid arachidonic acid (AA), a precursor of eicosanoids, and glycerol (Dinh et al., 2002; Blankman et al., 2007; Labar et al., 2009; Long et al., 2009a,b). This is evidenced by the observations where inhibition of MAGL by a selective and potent inhibitor JZL184 dramatically elevates brain levels of 2-AG and decreases levels of AA and AA-derived prostaglandins (Blankman et al., 2007; Long et al., 2009a,b; Nomura et al., 2011). 2-AG functions as a retrograde messenger in regulation or modulation of synaptic transmission and plasticity (Alger, 2009; Heifets & Castillo, 2009; Kano et al., 2009), exhibits anti-inflammatory and neuroprotective properties (Arevalo-Martin et al., 2010; Bisogno, 2010; Centonze et al., 2007; Chen et al., 2011; Panikashvili et al., 2001; 2005; Scotter et al., 2010; Zhang& Chen, 2008), and promotes neurogenesis (Gao et al., 2010). Prostaglandins have been long known as important mediators in synaptic plasticity, inflammatory response and neurodegenerative diseases such as AD (Chen et al., 2002; Hein & O'Banion, 2009; Hensley, 2010). Recent evidence shows that a large proportion of prostaglandins derives from metabolites of 2-AG by MAGL (Nomura et al., 2011). This means that MAGL is crucial in regulating endocannabinoid and prostaglandin signaling that tunes neuroinflammatory and neurodegenerative processes in response various assaults in the brain. Indeed, it has been demonstrated that pharmacological or genetic inhibition of MAGL suppresses neuroinflammation, prevents neurodegeneration against harmful insults, enhances long-term synaptic plasticity, and improves spatial learning through cannabinoid receptor type 1 (CB1R)-mediated mechanisms (Chen et al., 2011; Pan et al., 2009; Du et al., 2011). Most recent studies show that MAGL inactivation suppresses endotoxin lipopolysaccharide (LPS)-induced neuroinflammation and prevents neurodegeneration in a mouse model of Parkinson's disease by decreasing AA and its downstream proinflammatory prostaglandins (Nomura et al., 2011). These previous studies suggest an important role of MAGL in maintaining homeostasis of brain function and keeping inflammatory response in check. Here we show that inhibition of MAGL significantly reduces neuropathology and improves synaptic and cognitive function in 5XFAD APP transgenic mice, a mouse model of AD (Oakley et al., 2006), suggesting that MAGL is a promising therapeutic target for preventing and treating AD.

Results

MAGL inhibition prevents and decreases synthesis and accumulation of A β and expression of BACE1

Evidence from human AD and animal model studies supports a role of β-amyloid (Aβ) as the initiator in the etiology and pathogenesis of AD (Walsh & Selkoe, 2004; Ashe & Zahs, 2010). To determine the capability of MAGL inactivation in suppressing production and accumulation of Aβ, we used 4-nitrophenyl 4-(dibenzo[d][1,3]dioxol-5-

yl(hydroxy)methyl)piperidine-1-carboxylate (JZL184), a highly selective and potent MAGL inhibitor, which robustly elevates the levels of 2-AG and reduces AA in the brain (Long et al., 2009a,b; Schlosburg et al., 2010),. 5XFAD APP transgenic (TG) mice were used as the animal model of AD. As reported previously (Oakley et al., 2006; Kimura & Ohno, 2009), these mice rapidly recapitulate major features of AD amyloid pathology. Aβ is observed starting at 2 months of age, and amyloid plaques appear at 4 months of age, and a significant increase in amyloid plaques occurs at 5 to 6 months of age accompanied with synaptic and cognitive deficits. To determine whether inhibition of MAGL prevents and reduces synthesis of Aβ and deposition of Aβ plaques, we used two dosing regimes to treat TG animals with JZL184 (12 mg/kg, i.p.) three times per week starting at 2 months of age for 16 weeks or starting at 4 months of age for 8 weeks. Brain Aβ was detected at 6 months of age. The rationale for choosing this dosing regime is that JZL184 inhibits MAGL by irreversible active-site carbamoylation and 75% of MAGL is inhibited at a dose of 4 mg/kg and a near-complete blockade of MAGL occurs at a dose of 16 mg/kg (Long et al., 2009a,b). As shown in Supplementary Figs. S1 and S2, MAGL inhibition for 16 weeks robustly decreased total Aβ and Aβ42 as well as APP c-terminal fragments (CTFα/β) both in the cortex and hippocampus. We also found that expression of BACE1, the key enzyme for synthesis of neurotoxic Aβ1–42, was significantly suppressed in TG animals that received JZL184 for 16 weeks (Fig. S2). Of significance, TG animals treated with JZL184 (12 mg/kg, i.p.) three times per week starting at 4 months of age for 8 weeks also displayed significant decreases in total Aβ, Aβ42, CTFα/β, and BACE1 in both the cortex and hippocampus (Figs. 1 and 2), similar to those in animals treated for 16 weeks. These results suggest that inactivation of MAGL for 8 weeks is sufficient to decrease production and deposition of total Aβ and Aβ42 and expression of BACE1.

MAGL inactivation suppresses microglial and astrocytic activation and prevents neurodegeneration

Neuroinflammation is one of the major pathogenetic mechanisms that in concert lead to synaptic and cognitive deficits in AD. Astrocytes and microglia, which produce pro-inflammatory cytokines, chemokines and the complement system, are the characteristic components of the inflammatory response. To determine whether inhibition of MAGL prevents activation of astroglial cells, we determined reactive astrocytes and microglia using specific markers in TG animals that received JZL184 for 8 weeks. We found that JZL184 reduced reactive astroglial cells in the cortex and hippocampus of TG mice (Fig. 3a, b, c), indicating that neuroinflammation was suppressed when MAGL is inhibited.

Neurodegenerative changes are an important feature of neuropathology in AD. To determine whether MAGL inhibition reduces neurodegeneration, we stained brain slices with Fluoro-Jade C (FJC, a neurodegenerative marker) in TG animals that received JZL184 and observed that FJC positive neurons in the brain were significantly decreased in both TG mice treated with JZL184 for 16 weeks (Fig. 3d and 3e1) and 8 weeks (Fig. 3e2).

MAGL inhibition maintains integrity of hippocampal synaptic structure and function

It is generally accepted that deficits in structure and function of synapses are primary events in the early stages of AD and synaptic loss has been correlated with cognitive deficits in AD patients (DeKosky & Scheff, 1990; Selkoe, 2002). To determine whether MAGL inhibition prevents abnormality of hippocampal synapses in AD animals, we detected morphology of dendritic spines of pyramidal neurons in the CA1 region and granule neurons in the dentate gyrus using a two-photon laser scanning microscope in TG mice crossed bred with principal neuron-specific GFP transgenic mice (Feng et al., 2000). As seen in Fig. 4a, the density of total and mushroom dendritic spines of both hippocampal CA1 pyramidal neurons and dentate granule neurons were significantly reduced in TG mice when compared to that in

WT animals. However, the abnormality of spines was prevented in TG animals that received JZL184 for 8 weeks (Fig. 4a). In particular, the reduced density of mushroom spines was returned to the control level in JZL184-treated TG mice. Interestingly, the density of mushroom spines, where AMPA and NMDA receptors are primarily expressed and important for synaptic plasticity, was increased in WT animals treated with JZL184 when compared with vehicle-treated WT mice (Fig. 4a), suggesting that MAGL inactivation promotes neurite growth in dendrites.

AMPA and NMDA receptors in excitatory synapses are critical for synaptic transmission and plasticity. To determine whether MAGL inhibition diminishes the impaired expression of glutamate AMPA and/or NMDA receptor subunits in AD (Almeida et al., 2005; Battaglia et al., 2007; Hsieh et al., 2006), we detected expression of GluR1, GluR2, NR1, NR2A and NR2B in WT and TG animals. As shown in Fig. 4b and Fig. S3, expression of GluR1, GluR2, NR2A and NR2B both in the cortex and hippocampus was significantly reduced in TG mice, but the reduction was prevented in TG animals treated with JZL184 for 8 or 16 weeks. In particular, we observed that the expression levels of these subunits were greater in both JZL184 treated TG and WT animals compared to WT vehicle controls (Fig. 4b). This observation may underlie enhanced LTP and improved spatial learning in MAGL knockout mice (Pan et al., 2011). We also found that decreased expression of PSD-95, a post-synaptic marker, in TG mice was rescued by inhibition of MAGL (Fig. S3).

To determine whether MAGL inhibition, which prevented decreases in expression of hippocampal glutamate receptor subunits in TG animals, keeps functional normality of the glutamatergic synaptic transmission in TG animals, we recorded spontaneous excitatory postsynaptic currents (sEPSCs) in hippocampal CA1 pyramidal neurons. As shown in Fig. 4c, both frequency and amplitude of sEPSCs in TG mice were significantly reduced when compared to those in WT animals, consistent with the previous reports by others (Ting et al., 2007). Inhibition of MAGL resulted in increase in the amplitude of sEPSCs both in TG and WT animals, but not in the frequency. The reduced frequency and amplitude of sEPSCs are likely associated with the loss of presynaptic terminals and/or vesicular release at terminals (Mucke et al., 2000; Nimmrich, V. & Ebert, 2009) and decreased expression of postsynaptic glutamate receptor subunits in Aβ over-produced animals (Almeida et al., 2005; Battaglia et al., 2007; Hsieh et al., 2006).

Synaptic failure in AD is largely reflected by impaired long-term synaptic plasticity in terms of long-term potentiation (LTP). To further determine whether MAGL inhibition improves basal synaptic transmission and long-term synaptic plasticity in TG mice, we determined input-output function and LTP both at Shaffer-collateral synapses in the CA1 region and at perforant path synapses in the dentate gyrus (DG) of the hippocampus. As shown in Fig. 5a&b and Fig. S4, input-output function in both CA1 and DG was robustly depressed in TG mice, but it returned to the normal control levels in TG mice treated with JZL184 for 8 or 16 weeks. Similarly, LTP in both CA1 and DG was impaired in TG mice, but the impairments were diminished in JZL184 treated animals (Fig. 5b and Fig. S4). Interestingly, input-output function and LTP were both enhanced in WT mice that received JZL184. This may be associated with the increased expression of AMPA and NMDA receptor subunits as shown in Fig. 4b and Fig. S3. It was reported before that Aβ enhances long-term depression LTD (Hsieh et al., 2006; Shankar et al., 2008). We detected LTD induced by DHPG, a metabotropic glutamate receptor agonist. As indicated in Fig. S5, while DHPG virtually did not induce LTD in WT animals at 6 months of age, it did induce LTD in TG mice at the same age. Inhibition of MAGL eliminated DHPG-induced LTD, suggesting that MAGL inhibition not only reverses impaired LTP, but also suppressed enhanced LTD in AD animals.

A recent report shows that repeated injections of JZL184 with a higher dosage (40 mg/kg) once a day for 7 consecutive days causes functional tolerance and desensitization of brain CB1 receptors (Schlosburg et al., 2010). To determine whether repeated injections of JZL184 alter the expression and function of CB1 receptors, we recorded the synaptic response to exogenous application of synthetic cannabinoid WIN55,212-2 (WIN) and detected expression of CB1 receptors in the hippocampus. As shown in Fig. S6, repeated injections of JZL184 did not significantly alter hippocampal synaptic response to WIN and expression of CB1 receptors. To determine whether repeated injections of JZL184 causes a desensitization on its inhibitory effect on MAGL, we detected the brain levels of 2-AG, AA, and PGE_2 4 hrs after JZL184 (12 mg/kg, *i.p.*) injection in TG mice that had received JZL184 for 8 weeks. JZL184 injection increased 2-AG by 615.9±35.5% (vehicle control: 17.63±1.15 ng/mg *versus* JZL184: 108.45±6.27 ng/mg, n=8~10, P<0.01) and reduced AA by 76.5±1.8% (vehicle control: 19.83±0.80 ng/mg *versus* JZL184: 4.64±0.35 ng/mg, n=8~10, P<0.01), and PGE_2 by 40.7±3.9% (vehicle control: 3.55±0.21 pg/mg *versus* JZL184: 2.09±0.14 pg/mg, n=8~10, P<0.01) in TG mice. These results suggest that the dosing regime we used did not significantly induce functional tolerance of the endocannabinoid system including MAGL thus is feasible for the chronic treatment to inactivate MAGL.

MAGL inhibition improves spatial learning and memory

The most striking symptoms of AD are cognitive deficits. To determine whether inhibition of MAGL improves spatial learning and memory in TG mice treated with JZL184, we used the Morris water maze test. As shown in Fig. 6a&b and Fig. S7a&b, while TG mice treated with the vehicle took longer time to reach the hidden platform, those treated with JZL184 either for 8 or 16 weeks performed at WT control levels. In a probe trial, the number of crossing the target zone and time stayed in the target quadrant were significantly increased in TG mice treated with JZL184 when compared with the vehicle control (Fig. 6c&d and Fig. S7c&d). These results suggest that MAGL inactivation is capable of preventing memory deterioration in AD animals. In addition, WT mice treated with JZL184 exhibited enhanced spatial learning and memory (Fig. 6). This is consistent with the recent report showing that mice deficient in MAGL display improved spatial learning and memory (Pan et al., 2011).

MAGL inactivation-suppressed neuroinflammation is not mediated via CB1R or CB2R—Recent evidence shows that anti-inflammatory and neuroprotective effects by pharmacological and genetic inhibition of MAGL are not mediated by CB1R or CB2R (Normura et al., 2011; Piro et al., 2012). To determine whether JZL184-induced decrease in neuroinflammation is mediated by CB1R or CB2R, we created 5XFAD TG mice lacking CB1R or CB2R by crossed breeding 5XFAD transgenic mice with CB1KO or CB2KO mice. As shown in Figure 7, expression of GFAP was still reduced in both TG-CB1R KO and TG-CB2R KO mice treated with JZL184 for 8 weeks, suggesting that JZL184-produced suppression of neuroinflammation in APP TG mice may be mediated neither through the CB1R nor through the CB2R. This is consistent with the reports by others (Normura et al., 2011; Piro et al., 2012).

Discussion

We show here that inhibition of MAGL by JZL184 for 8 weeks robustly reduces production and accumulation of total Aβ and Aβ42, significantly decreases levels of activated astroglial markers and the number of degenerated neurons, maintains hippocampal synaptic structural and functional integrity, and retains normal learning and memory in 5XFAD APP transgenic mice. These discoveries indicate that inactivation of MAGL in a short period of time is sufficient to prevent pathogenesis and counteract neuropathology of AD and improve

synaptic and cognitive function. We also reveal that MAGL inactivation for 8 weeks results in increases in expression of glutamate AMPA and NMDA receptor subunits, hippocampal basal synaptic transmission and LTP, and improvements in spatial learning and memory in normal wild-type animals. Our results may underlie the recent observations showing enhanced hippocampal LTP and improved learning and memory via a CB1 receptor-dependent mechanism in MAGL null mice (Pan et al., 2011), revealing a previously unidentified role of MAGL in synaptic plasticity, learning and memory.

Function of MAGL was originally found to metabolize monoacylglycerol, a metabolite of triacylglycerol hydrolyzed by triacylglycerol lipase and hormone sensitive lipase, in the adipose tissue (Labar et al., 2010; Zechner et al., 2009). It is now known that MAGL is also expressed in many other tissues such as in cancer cells and in the brain (Dinh et al., 2002; Blankman et al., 2007; Nomura et al., 2010). In particular, recent studies identified and confirmed that MAGL is the primary enzyme degrading 2-AG (Hohmann et al., 2005; Blankman et al., 2007; Long et al., 2009a,b). It has been demonstrated that 85% of brain 2-AG is hydrolyzed by MAGL (the rest of 2-AG appears to be hydrolyzed by ABHD6 and ABHD12 (Blankman et al., 2007; Marrs et al., 2010), and oxidatively metabolized by COX-2 when expression and activity of COX-2 are excessively elevated during inflammation (Rouzer & Marnett, 2008). 2-AG, the most abundant endogenous cannabinoid and a full agonist for both CB1/2 receptors (Sugiura et al., 2006), possesses significant anti-inflammatory and neuroprotective effects in response to harmful insults (Arevalo-Martin et al., 2010; Chen et al., 2011;Du et al., 2011; Marsicano & Lutz, 2006; Panikashvili, et al., 2001; 2005; Zhang & Chen, 2008). 2-AG is also an agonist for peroxisome proliferator-activated receptors (PPARγ) (Du et al., 2011; O'Sullivan, 2007), which have been shown to protect neurons against Aβ toxicity and degeneration (Chen et al., 2011; Du et al., 2011; Kummer & Heneka, 2008), suggesting that 2-AG is an important endogenous signaling molecule 'on demand', responsible for maintaining homeostasis of brain function. For instance, the release of 2-AG is significantly increased in response to acute brain administration of Aβ42 in normal animals (van der Stelt et al., 2006). Expressions of the enzyme synthesizing 2-AG and MAGL are also altered in the senile plaque areas of human AD brains (Mulder et al., 2011), suggesting that enhanced 2-AG signaling is likely a homeostatic mechanism in counteracting neuropathology of AD. Recent studies reveal that MAGL inactivation suppresses inflammatory cytokines in LPS-treated animals and reduces neurodegeneration in MPTP model of Parkinson's disease by decreasing AA and PGE2 (Nomura et al., 2011). We and others (Piro et al., 2012) also observed that inhibition of CB1R or CB2R failed to prevent MAGL inactivation-reduced neuroinflammation in AD animals, suggesting that the suppressed neuroinflammatory response may be independent on CB1R or CB2R. Aβ is the initiator in the pathogenesis of AD (Ashe & Zahs, 2010; Walsh & Selkoe, 2004). It is likely that BACE1 inhibition-decreased synthesis and accumulation of Aβ by MAGL inactivation, which elevates levels of brain 2-AG and reduces AA and proinflammatory prostaglandins, may be crucial in reducing Aβ neuropathology and improving synaptic and cognitive function in AD animals. While 2-AG-produced beneficial effects in pathogenesis of AD may not be mediated by CB1R or CB2R, we cannot exclude the possibility that 2-AG may elicit its effects through the PPAR signaling pathway (O'Sullivan, 2007). In addition, improved synaptic transmission and long-term potentiation and enhanced spatial learning and memory by chronic MAGL inactivation in WT animals may be associated with the increased expression of glutamate receptor subunits and density of mushroom spines in the hippocampus. Although the mechanisms responsible for the MAGL inhibition-enhanced synaptic plasticity and spatial learning in normal control animals remain to be determined, the results obtained in the present study together with another report (Pan et al., 2011) suggest that the MAGL-regulated lipid signaling is involved in synaptic and cognitive function.

While significant progress has been made in the past decades in identifying and developing therapeutic interventions, we still lack FDA approved effective medications in delaying the onset of or preventing AD, and slowing, halting, or reversing the progressive decline in cognitive function and modifying the behavioral symptoms in AD. The results demonstrated in this report show that inhibition of MAGL by JZL184 for a short period of time using a dosing regime that does not induce functional tolerance of the endocannabinoid system results in significantly diminished amyloid neuropathology, reduced neuroinflammation and degeneration, and improved synaptic and cognitive function in AD animals. This indicates that MAGL, which regulates 2-AG and eicosanoid signaling in the brain, is an important locus in pathogenesis and neuropathology of AD, which is not previously revealed. While the molecular mechanisms responsible for the MAGL inhibition-produced beneficial effects against neuropathology of AD remain to be determined, our results suggest that MAGL would be a novel and promising therapeutic target for the prevention and treatment of AD and that identification and development of agents that target MAGL with high selectivity and potency will be a new direction for the AD therapeutic intervention.

Materials and Methods

Animals and chemicals

5XFAD transgenic (TG) mice, expressing both mutant human APP(695) with the Swedish (K670N, M671L), Florida (I716V), and London (V717I) Familial Alzheimer's Disease (FAD) mutations and human PS1 harboring two FAD mutations, M146L and L286V (Oakley et al., 2006), were obtained from the Jackson Lab (Stock number: 006554). As reported previously, these mice rapidly recapitulate major features of AD amyloid pathology, and intraneuronal Aβ42 is observed starting at 2 months of age. Aβ plaques appear at 4 months of age, and a significant increase in amyloid plaques occurs at 5 to 6 months of age accompanied with synaptic and cognitive deficits (Oakley et al., 2006; Kimura & Ohno, 2009; Zhao et al., 2007). Both female TG and age-matched wild-type (WT) littermates were used in the present study. APP TG-GFP transgenic mice were generated by 5XFAD mice crossed bred with principal neuron-specific GFP transgenic mice (Feng et al., 2000). APP TG-CB1 and -CB2 knockout (KO) mice were generated by 5XFAD mice crossing with CB1 (provided by NIHMH transgenic core) or CB2 (Jackson Lab) KO mice. The care and use of the animals reported in this study were approved by the Institutional Animal Care and Use Committee of Louisiana State University Health Sciences Center. JZL184 was purchased from Cayman Chemical and dissolved in the vehicle containing Tween-80 (10%), DMSO (10%) and saline (80%). To determine whether MAGL inhibition is capable of preventing pathogenesis and Aβ neuropathology, we treated TG mice with vehicle or JZL184 (12 mg/kg) three times per week by intraperitoneal (i.p.) starting at 2 months of age for 16 weeks or starting at 4 months of age for 8 weeks. All the observations and measurements in mice were made at 6 months of age.

Hippocampal slice preparation

Hippocampal slices from mice treated with vehicle or JZL184 were prepared as described previously (Chen et al., 2002; Fan et al., 2010). Briefly, after decapitation, brains were rapidly removed and placed in cold oxygenated (95% O_2, 5% CO_2) artificial cerebrospinal fluid (ACSF) composed of (in mM) 125.0 NaCl, 2.5 KCl, 1.0 $MgCl_2$, 25.0 $NaHCO_3$, 1.25 NaH_2PO_4, 2.0 $CaCl_2$, 25.0 glucose, 3.0 pyruvic acid, and 1.0 ascorbic acid. Slices were cut at a thickness of 350–400 μm and transferred to a holding chamber in an incubator containing oxygenated ACSF containing 3 pyruvic acid and 1 ascorbic acid at 36 °C for 0.5 to 1 hour, and then maintained in an incubator containing oxygenated ACSF at room temperature (~22–24 °C) for >1.5 hr before recordin gs. Slices were then transferred to a

recording chamber where they were continuously perfused with 95% O_2, 5% CO_2-saturated standard ACSF at ~32–34 °C.

Electrophysiological recordings

Field EPSP (fEPSP) recordings were made in response to stimulation at Shaffer-collateral synapses in the CA1 region or perforant path synapses in the dentate gyrus of the hippocampus at a frequency of 0.05 Hz using an Axoclamp-2B patch-clamp amplifier in bridge mode. Recording pipettes were pulled from borosilicate glass with a micropipette puller and filled with artificial ACSF (2–4 MΩ). Hippocampal LTP was induced by a theta-burst stimulation (TBS), consisting of a series of 10 bursts of 5 pulses at 100 Hz (200 ms interburst interval, which was repeated three times at 5-sec intervals (Fan et al., 2010). The input-output function was tested before recording of LTP, and the baseline stimulation strength was set to provide fEPSP with an amplitude of ~30% from the sub-threshold maximum derived from the input-output function. A paired-pulse protocol with varying interpulse intervals was used to determine paired-pulse ratio (PPR).

Spontaneous EPSCs (sEPSCs) were recorded in pyramidal neurons in hippocampal slices under a voltage clamp using an Axopatch-200B amplifier as described previously (Sang et al., 2005; Fan et al., 2010). Recording pipettes (2–4 MΩ) were pulled from borosilicate glass with a micropipette puller. The internal pipette solution contained (in mM) 115.0 Cs gluconate, 15.0 CsCl, 4.0 NaCl, 10.0 HEPES, 0.5 EGTA, 4.0 Mg_2ATP, and 0.5 Na_2GTP (pH 7.25 with CsOH). The membrane potential was held at −70 mV. The frequency, amplitude, and kinetics of sEPSCs were analyzed using the MiniAnalysis program. The bath solution contained bicuculline (10 μM).

Immunoblot

Western blot assay was conducted to determine production of Aβ and expression of BACE1, PSD-95 and glutamate receptor subunits in the brain from WT and TG mice treated with vehicle or JZL184. Cortical or hippocampal tissue was extracted and immediately homogenized in RIPA lysis buffer and protease inhibitors, and incubated on ice for 30 min, then centrifuged for 10 min at 10,000 rpm at 4oC. Supernatants were fractionated on 4-15% SDS-PAGE gels (Bio-Rad) and transferred onto PVDF membranes (Bio-Rad). The membrane was incubated with anti-Aβ42 (1:1,000, Invitrogen), anti-BACE1 (1:1000, Covance), Anti-PSD-95 (1:1000, Millipore), anti-GluR1 (1:1,000), GluR2 (1:1,000), NR1 (1:500), NR2A, NR2B (1:1,000, Millipore, Temecula, Ca) at 4°C overnight. The blots were washed and incubated with a secondary antibody (goat anti-rabbit 1:2,000, Cell Signaling, Danvers, MA) at room temperature for 1 hr. Proteins were visualized by enhanced chemiluminescence (ECL, Amersham Biosciences, UK). The densities of specific bands were quantified by densitometry using FUJIFILM Multi Gauge software (version 3.0). Band densities were normalized to the total amount of protein loaded in each well as determined by mouse anti β-actin (1:4000, Sigma) as described previously (Chen et al., 2011; Du et al., 2011; Zhang & Chen, 2008).

Immunohistochemistry

Immunohistochemical analyses were performed to determine total Aβ and Aβ1–42, astrocytic and microglial markers in coronal sectioned brain slices. Mice that received vehicle or JZL184 for 8 or 16 weeks at 6 months of age were anesthetized with ketamine/Xylazine (200/10 mg/kg) and subsequently transcardially perfused with PBS followed by 4% paraformaldehyde in phosphate buffer. The brains were quickly removed from the skulls and fixed in 4% paraformaldehyde overnight, and then transferred into the PBS containing 30% sucrose until sinking to the bottom of the small glass jars. Cryostat sectioning was made on a freezing Vibratome at 40 μm and series sections (10 to 12 slices) were collected

in 0.1M phosphate buffer. Free floating sections were immunostained using antibodies specific for total Aβ (4G8, 1:2,000, Invitrogen) and Aβ42 (1:2,000, Invitrogen), astrocytes (GFAP, 1:200, NeuroMab), microglial (F4/80 or OX42/CD11b, 1:200, Abcam) followed by incubation with the corresponding fluorescent-labeled secondary antibody. 4′-6-Diamidino-2-phenylindole (DAPI), a fluorescent stain that binds strongly to DNA, was used it to detect cell nuclei in the sections. The sections were then mounted on slides for immunofluorescence detection using a Zeiss deconvolution microscope with SlideBook 5.0 software. The imaging data were analyzed and quantified using SlideBook 5.0 and NIH Image J software.

Histochemistry

Degenerated neurons were detected using Fluoro-Jade C (FJC), which is an anionic dye that specifically stains the soma and neurites of degenerating neurons and thus is unique as a neurodegenerative marker. Cryostat cut sections were incubated in the solution with FJC (0.0001% solution, Millipore) and DAPI (0.5 μg/ml) for 10 min, followed by 3× 1-min wash with distilled water. Slices were dried naturally at room temperature without light. The images were taken using a Zeiss deconvolution microscope with SlideBook 5.0 software. FJC positive neurons were counted using Image J.

Two-photon imaging

Morphology of dendritic spines in hippocampal CA1 pyramidal neurons and dentate granule neurons was determined in WT and APP TG-GFP-expressing transgenic mice treated with vehicle and JZL184 using a two-photon laser scanning microscope (Chameleon hands-free ultrafast Ti: sapphire laser with an Olympus scan head) with FLUOVIEW 300 software, Olympus). Shape (thin, mushroom, or stubby), size, density, and volume of spines were measured from the three-dimensional reconstructions (Z stacks: 1 μ step for the whole cell and 0.1 μ step for a segment of dendrites) using 3D deconvolution plugin of Image J (http://bigwww.epfl.ch/algorithms/deconvolutionlab) and NeuronStudio (for 3D reconstruction of imaged dendritic spines, Version 0.9.92, http://research.mssm.edu/cnic/tools-ns.html). Spine densities were estimated by counting the number of spines along 100 to 150 μm (CA1) and 50 to 100 μm (DG) segments of dendrites in hippocampal neurons.

Liquid Chromatography/Mass Spectrometry

The amounts of 2-AG, AA, and PGE2 in brain tissues from TG mice that received vehicle or JZL184 were determined at the Medical College of Wisconsin Mass Spectrometry Facility using chromatography-atmospheric pressure chemical ionization-mass spectrometry as described previously (Patel et al., 2003). Briefly, animals were sacrificed by decapitation after suffocation with CO_2 and brains were rapidly frozen in liquid nitrogen. Tissue samples were weighed and placed into borosilicate glass tubes containing 2 ml of acetonitrile with 2-AG, AA, and PGE_2 internal standards for extraction. Tissue was homogenized with a glass rod and sonicated for 2 hr. Samples were incubated overnight at −10°C to precipitate proteins. Samples were centrifu ged at 1,500g, and supernatants were removed to a new glass tube and evaporated to dryness under N2 gas. The samples were resuspended in 500 μl of methanol to recapture any lipids adhering to the glass tube, and dried again. Finally, lipid extracts were suspended in 20 μl of methanol, 5 μl of which was used for detecting and analyzing using liquid chromatography-electrospray ionization-mass spectrometry (Agilent 1100 LC-MSD, SL model). The samples were separated on a Kromasil 100 C18 column, 250 x 2.0mm 5um (Phenomenex, Torrance, CA) using water (A) and acetonitrile (B) containing 0.01% acetic acid as a mobile phase. The mobile phase gradient increased from 60% B to 85% B in 10 minutes, increased to 90% B in 15 minutes and then increased to 100% B in 5 minutes. The flow rate was 300ul/min. The detection was made in the negative mode for PGE_2 and positive mode for 2AG. The m/z 355, 351, 356, 348, 387 and 379 were

used for detection of PGE_2-d4, PGE_2, 2AG-d8 and 2AG, respectively. The samples were then diluted and analyzed for Arachidonic Acid (AA) using a different gradient. The mobile phase gradient started at 90% B and increased to 100% B in 15 minutes with a flow rate of 300ul/min. The detection was made in the negative mode. The m/z 311 and 303 were used for detection of AA-d8 and AA respectively. The concentrations of the analytes were calculated from the ratios of peak areas of compounds to internal standards as compared with the standard curves.

Behavioral tests

The classic Morris water maze test was used to determine spatial learning and memory. A circle water tank (diameter 100 cm and 75 cm in high) was filled with water and the water was made opaque with non-toxic white paint. A round platform (diameter 15 cm) was hidden 1 cm beneath the surface of the water at the center of a given quadrant of the water tank. Before hidden platform training, the mice were given 3 days of nonspatial training (4 trials per day) to find the submerged platform marked with a cue visible above the water line. Animals that failed to mount the platform were gently guided to it and allowed to stand on it for 10 sec. Invisible platform training was carried out continuous 7 days (7 sessions) and each session consisted of 4 trials. For each trial, the mouse was released from the wall of the tank and allowed to search, find, and stand on the platform for 10 seconds within the 60-second trial period. For each training session, the starting quadrant and sequence of the four quadrants from where the mouse was released into the water tank were randomly chosen so that it was different among the separate sessions for each animal and was different for individual animals. The mice in the water pool were recorded by a video-camera and the task performances, including swimming paths, speed, and time spent in each quadrant were recorded by using an EthoVision video tracking system (Noldus). A probe test was conducted 24 hours after the completion of the invisible training. During the probe test, the platform was removed from the pool, and the task performances will be recorded for 60 seconds. The time spent in each quadrant was analyzed.

Data analysis

Data are presented as mean ± S.E.M. Unless stated otherwise, analysis of variance (ANOVA) with Fisher's PLSD test or Bonferroni post-hoc test were used for statistical comparison when appropriate. Differences were considered significant when $P< 0.05$.

Acknowledgments

The authors thank NIH Mental Health Institute Chemical Synthesis and Drug Supply Program for providing compounds used in this study, NIMH transgenic core for providing CB1R knockout mice, and Ms. Marilyn Isbell at Medical College of Wisconsin for detecting lipids. This work was supported by National Institutes of Health grants R01NS076815, R01NS054886, and R21AG039669 (to C.C.).

References

Alger BE. Endocannabinoid signaling in neural plasticity. Curr Top Behav Neurosci. 2009; 1:141–172. [PubMed: 21104383]

Almeida CG, Tampellini D, Takahashi RH, Greengard P, Lin MT, Snyder EM, Gouras GK. Beta-amyloid accumulation in APP mutant neurons reduces PSD-95 and GluR1 in synapses. Neurobiol Dis. 2005; 20:187–198. [PubMed: 16242627]

Arevalo-Martin A, Garcia-Ovejero D, Molina-Holgado E. The endocannabinoid 2-arachidonoylglycerol reduces lesion expansion and white matter damage after spinal cord injury. Neurobiol Dis. 2010; 38:304–312. [PubMed: 20156559]

Ashe KH, Zahs KR. Probing the biology of Alzheimer's disease in mice. Neuron. 2010; 66:631–645. [PubMed: 20547123]

Battaglia F, Wang HY, Ghilardi MF, Gashi E, Quartarone A, Friedman E, Nixon RA. Cortical plasticity in Alzheimer's disease in humans and rodents. Biol Psychiatry. 2007; 62:1405–1412. [PubMed: 17651702]

Bisogno T, Di Marzo V. Cannabinoid receptors and endocannabinoids: role in neuroinflammatory and neurodegenerative disorders. CNS Neurol Disord Drug Targets. 2010; 9:564–573. [PubMed: 20632970]

Blankman JL, Simon GM, Cravatt BF. A comprehensive profile of brain enzymes that hydrolyze the endocannabinoid 2-arachidonoylglycerol. Chem Biol. 2007; 14:1347–1356. [PubMed: 18096503]

Centonze D, Finazzi-Agrò A, Bernardi G, Maccarrone M. The endocannabinoid system in targeting inflammatory neurodegenerative diseases. Trends Pharmacol Sci. 2007; 28:180–187. [PubMed: 17350694]

Chen C, Magee JC, Bazan NG. Cyclooxygenase-2 regulates prostaglandin E2 signaling in hippocampal long-term synaptic plasticity. J Neurophysiol. 2002; 87:2851–2857. [PubMed: 12037188]

Chen X, Zhang J, Chen C. Endocannabinoid 2-arachidonoylglycerol protects neurons against β-amyloid insults. Neurosci. 2011; 178:159–168.

DeKosky ST, Scheff SW. Synapse loss in frontal cortex biopsies in Alzheimer's disease: correlation with cognitive severity. Ann Neurol. 1990; 27:457–464. [PubMed: 2360787]

Dinh TP, Carpenter D, Leslie FM, Freund TF, Katona I, Sensi SL, Kathuria S, Piomelli D. Brain monoglyceride lipase participating in endocannabinoid inactivation. Proc Natl Acad Sci U S A. 2002; 99:10819–10824. [PubMed: 12136125]

Du H, Chen X, Zhang J, Chen C. Inhibition of COX-2 expression by endocannabinoid 2-arachidonoylglycerol is mediated via PPAR-γ. Br J Pharmacol. 2011; 163:1533–1549. [PubMed: 21501147]

Fan N, Yang H, Zhang J, Chen C. Reduced expression of glutamate receptors and phosphorylation of CREB are responsible for 9-THC-impaired hippocampal synaptic plasticity. J Neurochem. 2010; 112:691–702. [PubMed: 19912468]

Feng G, et al. Imaging neuronal subsets in transgenic mice expressing multiple spectral variants of GFP. Neuron. 2000; 28:41–51. [PubMed: 11086982]

Gao Y, et al. Loss of retrograde endocannabinoid signaling and reduced adult neurogenesis in diacylglycerol lipase knock-out mice. J Neurosci. 2010; 30:2017–2024. [PubMed: 20147530]

Heifets BD, Castillo PE. Endocannabinoid signaling and long-term synaptic plasticity. Annu Rev Physiol. 2009; 71:283–306. [PubMed: 19575681]

Hein AM, O'Banion MK. Neuroinflammation and memory: the role of prostaglandins. Mol Neurobiol. 2009; 40:15–32. [PubMed: 19365736]

Hensley K. Neuroinflammation in Alzheimer's disease: mechanisms, pathologic consequences, and potential for therapeutic manipulation. J Alzheimers Dis. 2010; 21:1–14. [PubMed: 20182045]

Hsieh H, Boehm J, Sato C, Iwatsubo T, Tomita T, Sisodia S, Malinow R. AMPAR removal underlies Abeta-induced synaptic depression and dendritic spine loss. Neuron. 2006; 52:831–843. [PubMed: 17145504]

Hohmann AG, et al. An endocannabinoid mechanism for stress-induced analgesia. Nature. 2005; 435:1108–1112. [PubMed: 15973410]

Kano M, Ohno-Shosaku T, Hashimotodani Y, Uchigashima M, Watanabe M. Endocannabinoid-mediated control of synaptic transmission. Physiol Rev. 2009; 89:309–380. [PubMed: 19126760]

Kimura R, Ohno M. Impairments in remote memory stabilization precede hippocampal synaptic and cognitive failures in 5XFAD Alzheimer mouse model. Neurobiol Dis. 2009; 33:229–235. [PubMed: 19026746]

Kummer MP, Heneka MT. PPARs in Alzheimer's disease. PPAR Res. 2008; 2008:1–8.

Labar G, Wouters J, Lambert DM. A review on the monoacylglycerol lipase: at the interface between fat and endocannabinoid signalling. Curr Med Chem. 2010; 17:2588–2607. [PubMed: 20491633]

Long JZ, Normura DK, Cravatt BF. Characterization of monoacylglycerol lipase inhibition reveals differences in central and peripheral endocannabinoid metabolism. Chem Biol. 2009; 16:744–753. [PubMed: 19635411]

Long JZ, et al. Selective blockade of 2-arachidonoylglycerol hydrolysis produces cannabinoid behavioral effects. Nat Chem Biol. 2009; 5:37–44. [PubMed: 19029917]

Marrs WR, et al. The serine hydrolase ABHD6 controls the accumulation and efficacy of 2-AG at cannabinoid receptors. Nat Neurosci. 2010; 13:951–957. [PubMed: 20657592]

Marsicano G, Lutz B. Neuromodulatory functions of the endocannabinoid system. J Endocrinol Invest. 2006; 29:27–46. [PubMed: 16751707]

Mucke L, et al. High-level neuronal expression of abeta 1–42 in wild-type human amyloid protein precursor transgenic mice: synaptotoxicity without plaque formation. J Neurosci. 2000; 20:4050–4058. [PubMed: 10818140]

Mulder J, et al. Molecular reorganization of endocannabinoid signalling in Alzheimer's disease. Brain. 2011; 134:1041–1060. [PubMed: 21459826]

Nimmrich V, Ebert U. Is Alzheimer's disease a result of presynaptic failure? Synaptic dysfunctions induced by oligomeric beta-amyloid. Rev Neurosci. 2009; 20:1–12. [PubMed: 19526730]

Nomura DK, et al. Endocannabinoid hydrolysis generates brain prostaglandins that promote neuroinflammation. Science. 2011; 334:809–813. [PubMed: 22021672]

Nomura DK, Long JZ, Niessen S, Hoover HS, Ng SW, Cravatt BF. Monoacylglycerol lipase regulates a fatty acid network that promotes cancer pathogenesis. Cell. 2010; 140:49–61. [PubMed: 20079333]

Panikashvili D, Simeonidou C, Ben-Shabat S, Hanus L, Breuer A, Mechoulam R, Shohami E. An endogenous cannabinoid (2-AG) is neuroprotective after brain injury. Nature. 2001; 413:527–531. [PubMed: 11586361]

Oakley H, et al. Intraneuronal β-amyloid aggregates, neurodegeneration, and neuron loss in transgenic mice with five familial Alzheimer's disease mutations: potential factors in amyloid plaque formation. J Neurosci. 2006; 26:10129–10140. [PubMed: 17021169]

O'Sullivan SE. Cannabinoids go nuclear: evidence for activation of peroxisome proliferator-activated receptors. Br J Pharmacol. 2007; 152:576–582. [PubMed: 17704824]

Pan B, Wang W, Long JZ, Sun D, Hillard CJ, Cravatt BF, Liu QS. Blockade of 2-arachidonoylglycerol hydrolysis by selective monoacylglycerol lipase inhibitor 4-nitrophenyl 4-(dibenzo[d][1,3]dioxol-5-yl(hydroxy)methyl)piperidine-1-carboxylate (JZL184) Enhances retrograde endocannabinoid signaling. J Pharmacol Exp Ther. 2009; 331:591–597. [PubMed: 19666749]

Pan B, Wang W, Zhong P, Blankman JL, Cravatt BF, Liu QS. Alterations of endocannabinoid signaling, synaptic plasticity, learning, and memory in monoacylglycerol lipase knock-out mice. J Neurosci. 2011; 31:13420–13430. [PubMed: 21940435]

Panikashvili D, Simeonidou C, Ben-Shabat S, Hanus L, Breuer A, Mechoulam R, Shohami E. An endogenous cannabinoid (2-AG) is neuroprotective after brain injury. Nature. 2001; 413:527–531. [PubMed: 11586361]

Panikashvili D, Mechoulam R, Beni SM, Alexandrovich A, Shohami E. CB1 cannabinoid receptors are involved in neuroprotection via NF-kappa B inhibition. J Cereb Blood Flow Metab. 2005; 25:477–484. [PubMed: 15729296]

Patel S, Rademacher DJ, Hillard CJ. Differential regulation of the endocannabinoids anandamide and 2-arachidonylglycerol within the limbic forebrain by dopamine receptor activity. J Pharmacol Exp Ther. 2003; 306:880–888. [PubMed: 12808005]

Piro JR, Benjamin DI, Duerr JM, Pi Y, Gonzales C, Wood KM, Schwartz JW, Nomura DK, Samad TA. A Dysregulated Endocannabinoid-Eicosanoid Network Supports Pathogenesis in a Mouse Model of Alzheimer's Disease. Cell Reports. 2012; 1:617–623. [PubMed: 22813736]

Rouzer CA, Marnett LJ. Non-redundant functions of cyclooxygenases: oxygenation of endocannabinoids. J Biol Chem. 2008; 283:8065–8069. [PubMed: 18250160]

Sang N, Zhang J, Marcheselli V, Bazan NG, Chen C. Postsynaptically synthesized prostaglandin E2 modulates hippocampal synaptic transmission via a presynaptic PGE2 EP2 receptor. J Neurosci. 2005; 25:9858–9870. [PubMed: 16251433]

Schlosburg JE, et al. Chronic monoacylglycerol lipase blockade causes functional antagonism of the endocannabinoid system. Nat Neurosci. 2010; 13:1113–1119. [PubMed: 20729846]

Scotter EL, Abood ME, Glass M. The endocannabinoid system as a target for the treatment of neurodegenerative disease. Br J Pharmacol. 2010; 160:480–498. [PubMed: 20590559]

Selkoe DJ. Alzheimer's disease is a synaptic failure. Science. 2002; 298:789–791. [PubMed: 12399581]

Shankar GM, et al. Amyloid-beta protein dimers isolated directly from Alzheimer's brains impair synaptic plasticity and memory. Nat Med. 2008; 14:837–842. [PubMed: 18568035]

Sugiura T, kishimoto S, Oka S, Gokoh M. Biochemistry, pharmacology and physiology of 2-arachidonoylglycerol, an endogenous cannabinoid receptor ligand. Prog Lipid Res. 2006; 45:405–446. [PubMed: 16678907]

Ting JT, Kelley BG, Lambert TJ, Cook DG, Sullivanm JM. Amyloid precursor protein overexpression depresses excitatory transmission through both presynaptic and postsynaptic mechanisms. Proc Natl Acad Sci U S A. 2007; 104:353–358. [PubMed: 17185415]

van der Stelt M, et al. Endocannabinoids and beta-amyloid-induced neurotoxicity *in vivo*: effect of pharmacological elevation of endocannabinoid levels. Cell Mol Life Sci. 2006; 63:1410–1424. [PubMed: 16732431]

Walsh DM, Selkoe DJ. Deciphering the molecular basis of memory failure in Alzheimer's disease. Neuron. 2004; 44:181–193. [PubMed: 15450169]

Zechner R, Kienesberger PC, Haemmerle G, Zimmermann R, Lass A. Adipose triglyceride lipase and the lipolytic catabolism of cellular fat stores. J Lipid Res. 2009; 50:3–21. [PubMed: 18952573]

Zhang J, Chen C. Endocannabinoid 2-arachidonoylglycerol protects neurons by limiting COX-2 elevation. J Biol Chem. 2008; 283:22601–20611. [PubMed: 18534982]

Highlights

1. Inactivation of MAGL reduces Aβ plaques and BACE1 expression in AD mice.
2. MAGL inhibition decreases neuroinflammation and neurodegeneration.
3. MAGL inhibition maintains integrity of hippocampal synaptic structure and function.
4. MAGL inhibition improves synaptic plasticity and learning and memory in AD mice

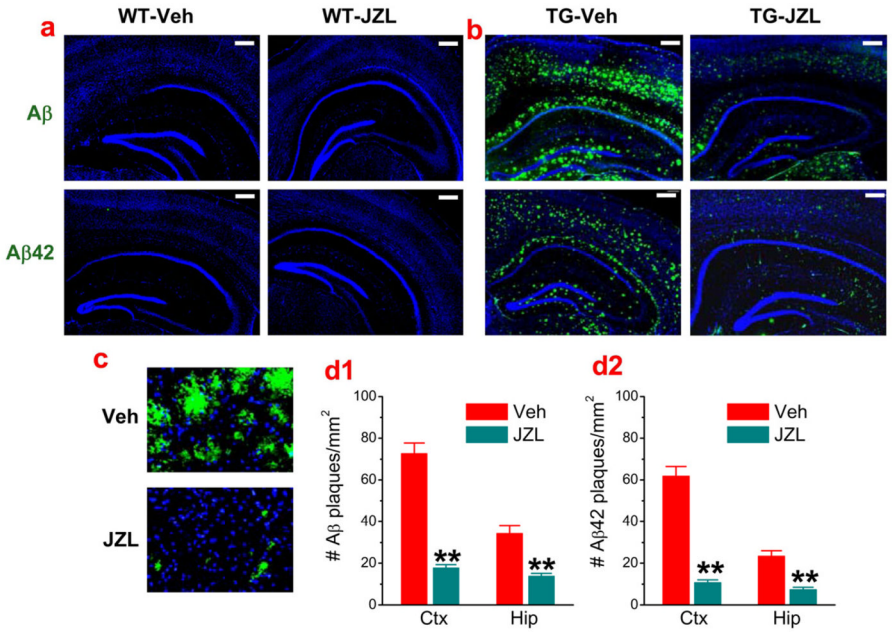

Figure 1.

MAGL inhibition reduces production and deposition of Aβ in 5XFAD APP transgenic (TG) mice. **a**, **b**, Accumulation and deposition of total Aβ (all forms) and Aβ42 in 6 months old TG and their age-matched WT mice that received the vehicle and JZL184 (12 mg/kg, i.p.) three times per week starting at 4 months of age for 8 weeks. Total Aβ and Aβ42 were detected using immunohistochemistry with antibodies specific for all forms of Aβ (4G8, green) and for Aβ42 (green). Cell nuclei in the sections were stained with DAPI (Blue). Scale Bars: 400 μm. **c**, Magnification of Aβ plaques in vehicle- and JZL-treated TG mice. **d**, Number of total Aβ and Aβ42 in the cortex and hippocampus in vehicle- and JZL-treated TG mice. Data are means ±SEM from 5 to 6 mice per group. **P<0.01 compared with the vehicle control.

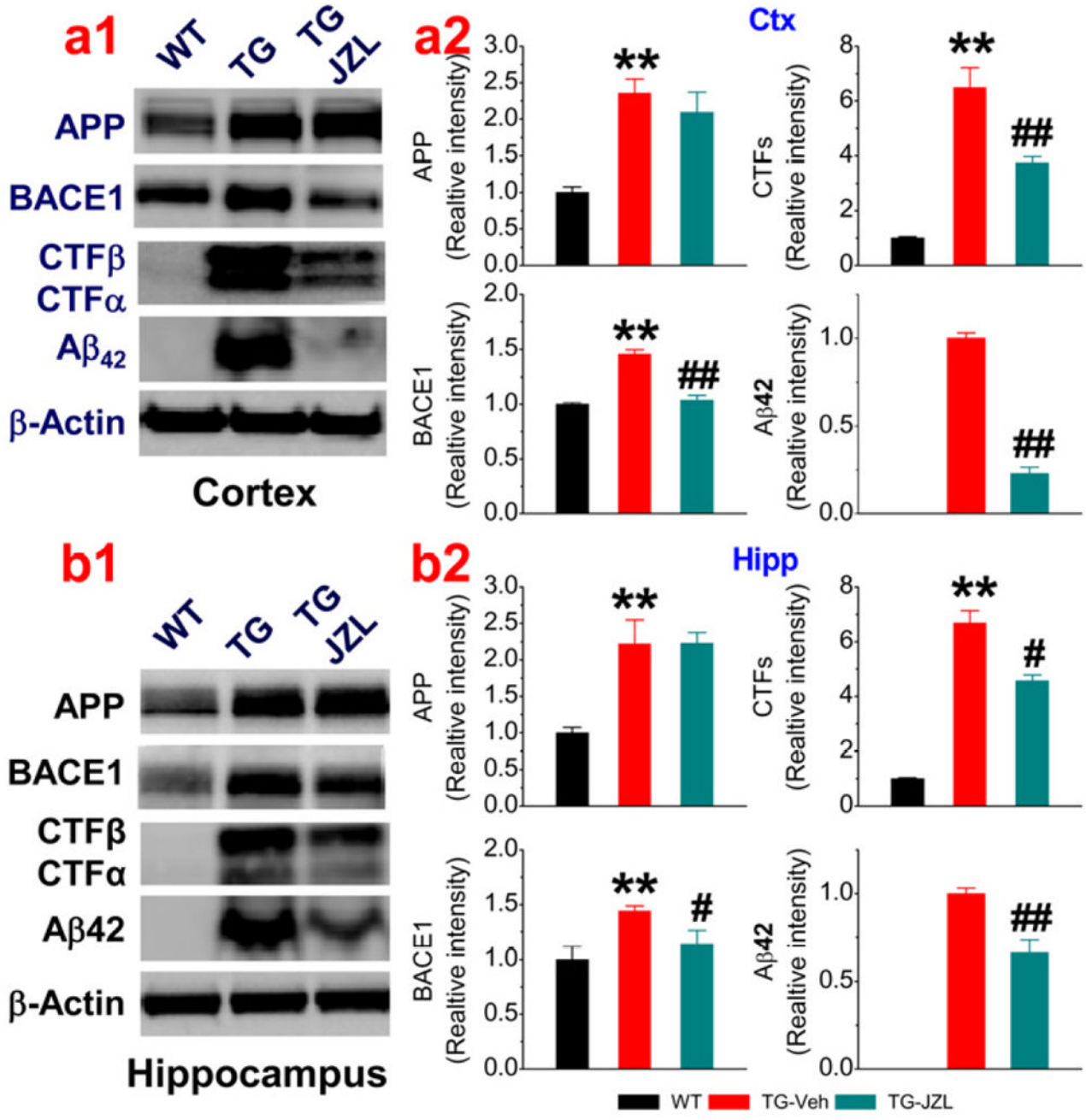

Figure 2.

MAGL inhibitor JZL184 decreases expression of BACE1 and production of Aβ in TG mice. **a**, Immunoblot analysis of APP, BACE1, CTFβ/α, and Aβ42 in the cortex in 6 months old TG and their age-matched WT mice treated with the vehicle and JZL184 for 8 weeks. **b**, Immunoblot analysis of APP, BACE1, CTFβ/α, and Aβ42 in the hippocampus in vehicle- and JZL-treated TG mice. Data are means ±SEM from 4 to 6 mice per group. **P<0.01 compared with the WT vehicle control; §§P<0.01 compared with the TG vehicle control.

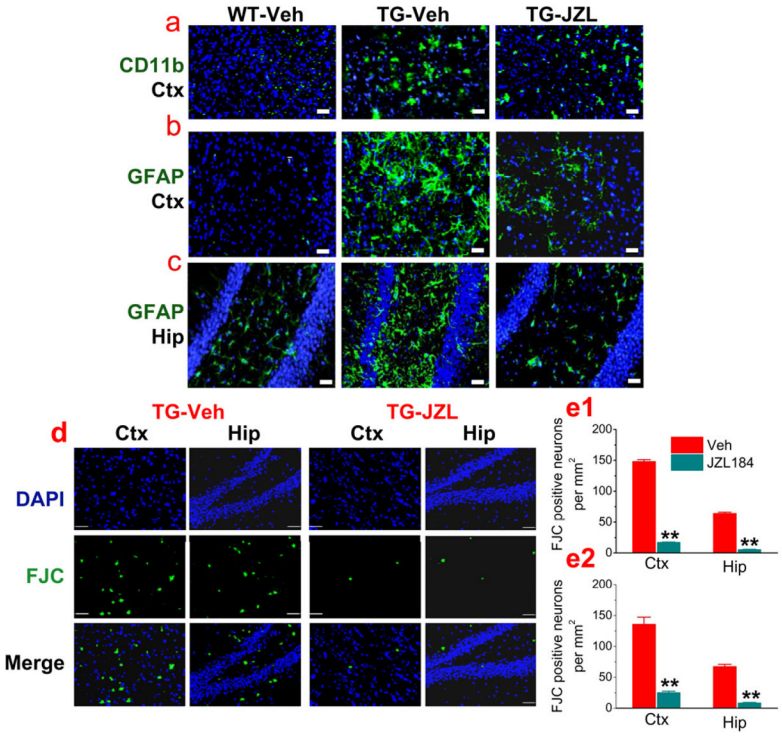

Figure 3.

MAGL inhibition prevents neuroinflammation and reduces neurodegeneration in TG mice. **a**, Reactive microglial cells (CD11b/OX42, a microglial marker, green) are suppressed in 6 month old TG mice treated with JZL184 for 8 weeks. Scale bars: 200 μm. **b**, **c**, Activated astrocytes (GFAP, an astrocytic marker, green) in the cortex and hippocampus are reduced in TG mice that received JZL184 for 8 weeks. Scale bars: 100 μm. **d**, **e**, Degenerated neurons (FJC, a neurodegeneration marker, green, DAPI: red) are reduced in the cortex and hippocampus in TG mice treated with JZL184 for 8 (**e1**) and 16 (**e2**) weeks. **P<0.01 compared with the TG vehicle control (Data are averaged from 3 to 4 sections in three groups of mice, n=4 mice per group).

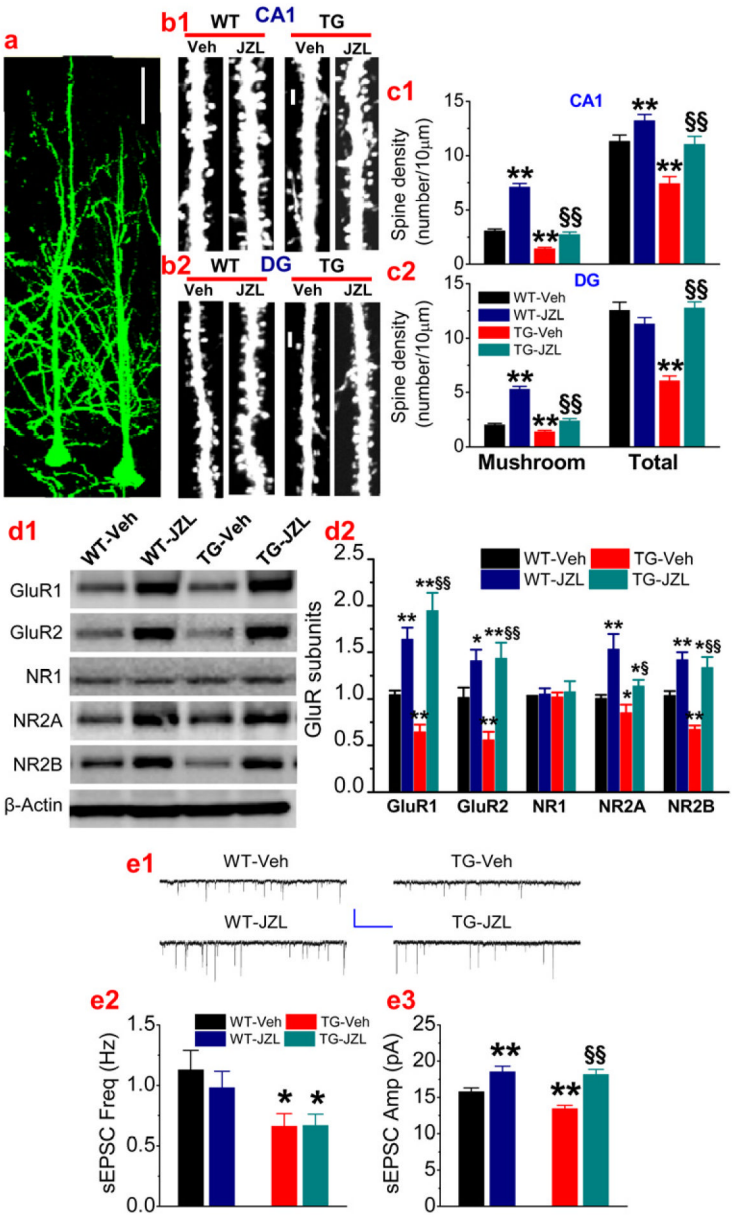

Figure 4.

MAGL inactivation maintains integrity of hippocampal synaptic structure and function in TG mice. **a**, Two-photon image of GFP-expressing pyramidal neurons in the hippocampus from a transgenic mouse that expresses GFP in principal neurons. Scale bar: 50 μm. **b**, Segments of dendrites of pyramidal neurons in the CA1 region (**b1**) and of granule neurons in the dentate gyrus (DG, **b2**) in 6 months old WT-GFP- and TG-GFP-expressing animals that received vehicle or JZL184 for 8 weeks. Scale bars: 2 μm. **c**, Density of mushroom and total dendritic spines in CA1 pyramidal neurons (**c1**) and DG granule neurons (**c2**). The data represent mean values averaged from 43 to 56 images/group and 5 to 7 mice/group. **P<0.01 compared with the WT vehicle control; §§P<0.01 compared with the TG vehicle control. **d**, Immunoblot analysis of hippocampal expression of AMPA (GluR1 and GluR2) and NMDA (NR1, NR2A and NR2B) receptor subunits in 6 months old WT and TG mice treated with vehicle or JZL184 for 8 weeks. **e**, Spontaneous excitatory postsynaptic currents

(sEPSCs) recorded in hippocampal CA1 pyramidal neurons in 6 months old WT and TG mice treated with vehicle or JZL184 for 8 weeks. Frequency and amplitude of sEPSCs were analyzed using the MiniAnalysis program. *P<0.05; **P<0.01 compared with the WT vehicle control, §P<0.05, §§P<0.01 compared with the TG vehicle control. 14 to 20 recordings were made in each group of animals (3 to 4 mice per group).

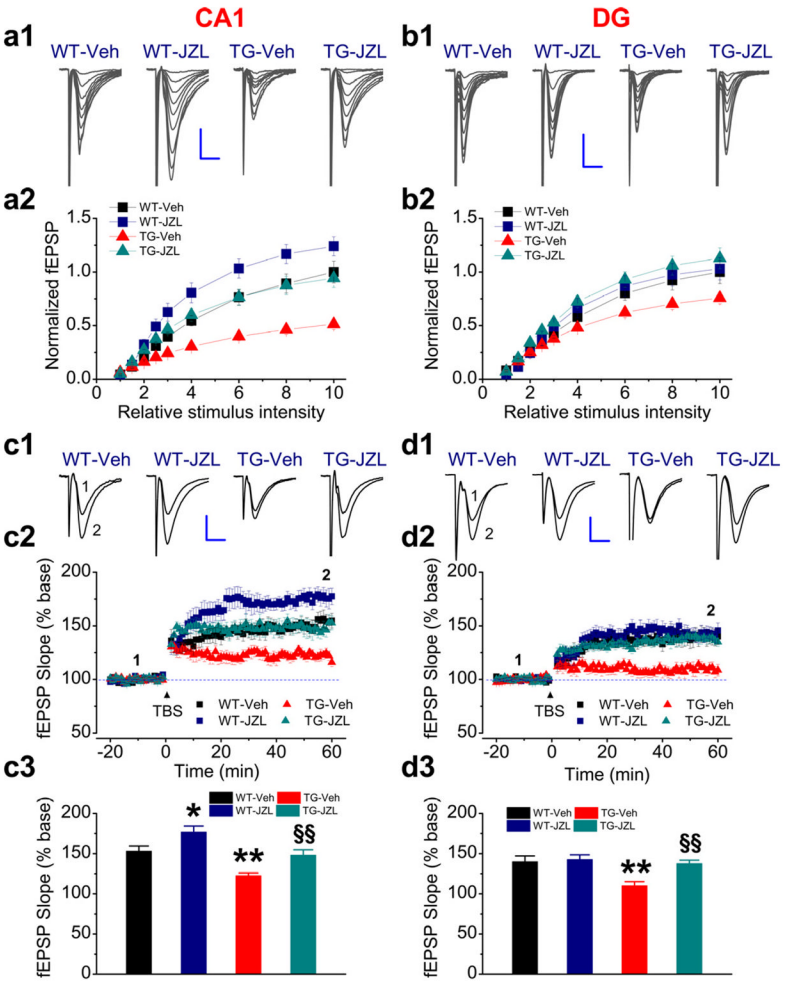

Figure 5.

MAGL inhibition improves basal synaptic transmission and long-term synaptic plasticity in both WT and TG mice. **a1**, **a2**, Representative fEPSP waveforms recorded at hippocampal CA3-CA1 synapses and input-output function in 6 months old WT and TG injected with vehicle or JZl184 for 8 weeks (16 to 22 recordings/group and 5 to 8 mice/group). **b1**, **b2**, Representative fEPSP waveforms recorded at perforant path synapses and input-output function in 6 months old WT and TG injected with vehicle or JZl184 for 8 weeks (15 to 16 recordings/group and 5 to 6 mice/group). Stimulus intensity was normalized to the maximum intensity. Scale bar: 0.3 mV/10 msec. **c1**–**c3**, Representative fEPSP waveforms recorded at hippocampal CA3-CA1 synapses, LTP curves and mean values of fEPSP slope averaged from 56 to 60 min following theta-burst stimulation (TBS) in 6 months old WT and TG injected with vehicle or JZl184 for 8 weeks (10 to 14 recordings/group and 7 to 8 mice/group). **d1**–**d3**, Representative fEPSP waveforms recorded at perforant path synapses, LTP curves and mean values of fEPSP slope averaged from 56 to 60 min following TBS in 6 months old WT and TG injected with vehicle or JZl184 for 8 weeks (10 to 13 recordings/group and 5 to 8 mice/group). *P<0.05; **P<0.01 compared with the WT vehicle control; §P<0.05, §§P<0.01 compared with the TG vehicle control.

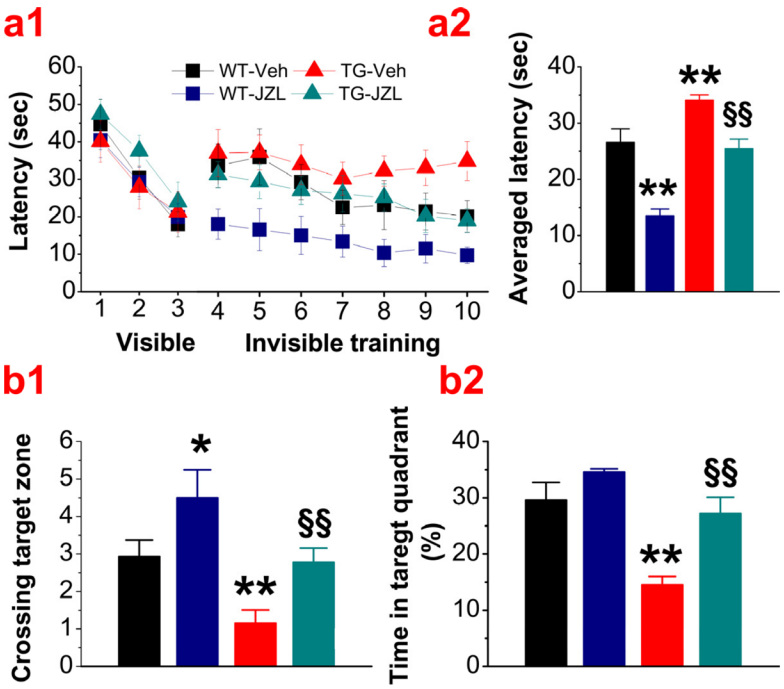

Figure 6.

MAGL inhibition prevents spatial learning and memory deterioration in TG mice and enhances spatial learning and memory in WT mice. **a**, Spatial learning in the Morris water maze in 6-month-old WT and TG mice that received vehicle or JZL184 for 8 weeks. The test was conducted one week following the cessation of the treatment. The submerged platform was located in the center of one quadrant of the pool. Mice received visible platform training for 3 days followed by 7 days of invisible platform training. **b**, Averaged latency in 7 days of invisible training. Retention memory was determined using a probe trial test conducted 24 hrs after 7 days of training. During the probe test, the platform was removed from the pool. **c**, Number of times crossing the target zone, and **d**, Percentages of time stayed in the target quadrant. *P<0.05, **<0.01, compared with the WT vehicle control; §P<0.05, §§P<0.01 compared with the TG vehicle (n=9 to 12 mice/group).

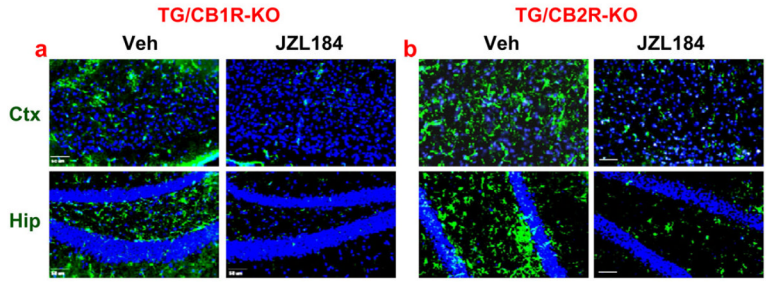

Figure 7.

MAGL inhibition-produced suppression of neuroinflammation is mediated neither by CB1R nor by CB2R in AD animals. 5XFAD transgenic mice were crossed with CB1 receptor knockout (CB1RKO) or CB2 receptor knockout mice (CB2RKO) to generate 5XFAD TG mice lacking CB1R or CB2R. **a & b**, Reactive astrocytes (GFAP, an astrocytic marker, green) are suppressed in 6 month old TG mice lacking CB1R or CB2R treated with JZL184 for 8 weeks. Scale bars: 50 μm.